

A Novel Single Frequency, Pulsed UV Source For Airborne Direct Detection Wind Lidar

Johann Thurn*, Raoul-Amadeus Lorbeer, Peter Mahnke, Matthias Damm, Oliver Kliebisch

Institute of Technical Physics, German Aerospace Center, Pfaffenwaldring 38-40, 70569 Stuttgart, Germany

**johann.thurn@dlr.de*

Abstract: We have conceptualized a compact UV source with pulse parameters optimized for airborne clear air turbulence detection. An amplified single frequency ns-Nd:YAG source is frequency-tripled to 355 nm, > 2.5 W at 3 kHz pulse repetition frequency. © 2022 The Author(s)

1. Introduction

Airborne lidar applications usually need highly specialized lasers to fit the specific requirements set by the chosen detection scheme while also fulfilling safety considerations for the measurement environment. Lasers often had to be developed specifically to fit these constraints. Prominent examples are the laser used in the AWIATOR project [1] for clear air turbulence (CAT) detection, the WALES system [2] for airborne water vapor detection, the laser of which was also used in the DELICAT project [3] or the laser for the ALADIN airborne demonstrator [4] which went spaceborne within the ADM-Aeolus mission [5].

We have now built a specialized master oscillator power amplifier (MOPA) demonstrator intended for a lidar system developed to enable gust load alleviation (GLA) capabilities for airborne vessels in CAT scenarios [6].

2. Amplifier System

The laser parameters are based on simulations and previous findings where a field-widened fringe-imaging michelson interferometer (FWFIMI) [6] has been developed for the wind measurement with a direct detection wind lidar (DD-DWL) via the Doppler shift. Optimal parameters highly depend on the planned lidar system. Next to many more these parameters are: 355 nm, < 0.5 GHz linewidth, 1-3 kHz PRF, 10 ns pulsewidth and > 2.5 W output power. While most parameters can easily be fulfilled, it is difficult to build a single longitudinal mode (SLM) laser with inherently high output power and high pulse energy while balancing size, weight and power requirements for compact airborne integration. For that reason it is most advantageous to start with a laser capable of fulfilling most requirements but low power and amplify the pulses to the needed energy.

Depending on the master oscillator (MO) it may be necessary to employ more than one amplification stage. Considering availability and size we have opted to start with a Nd:YAG microchip laser (20 μ J pulse energy, Teem Photonics) and amplify it in two stages. The first stage uses a Nd:YAG single crystal fiber (SCF, 0.2 at %, Fibercryst) in double pass configuration and is end-pumped with 808 nm, 15 W. The second stage shown in Fig. 1 uses a self-designed segmented Nd:YAG rod in double-pass configuration with three doping concentrations and endcaps to counter thermal effects [7]. It is end-pumped with 808 nm, up to 200 W and directly water-cooled in a self-designed cooling block. The amplified pulses are then to be frequency-tripled in two temperature-controlled LBO-crystals (Eksma Optics).

The expected amplified pulse energy was calculated for both stages using a simple Frantz-Nodvik model [8]. For the SCF amplifier $\sim 700 \mu$ J and for the second stage ~ 15 mJ were calculated assuming ideal conditions. The conversion efficiency to 355 nm can reasonably be expected to exceed 25 % [9].

3. Results

The 20 μ J, 3 kHz pulses from the microchip laser were amplified to a pulse energy of 500 μ J using only the SCF amplifier stage with 15 W pump power which is reasonably close to the expected pulse energy. With 10 % this is below the advertised 30 % extraction efficiency, but well within our expectations, as the amplifier is not driven in saturation.

The second stage optics (mirrors, isolator, TFP, dichroics) introduce loss of about 20 % in total so that we have $\sim 400 \mu$ J of pulse energy at the entrance facet of the second stage. In first trials, we diverged from ideal conditions to larger pump spots with lower pump powers up to 70 W to approach higher pump fluences within the amplifier

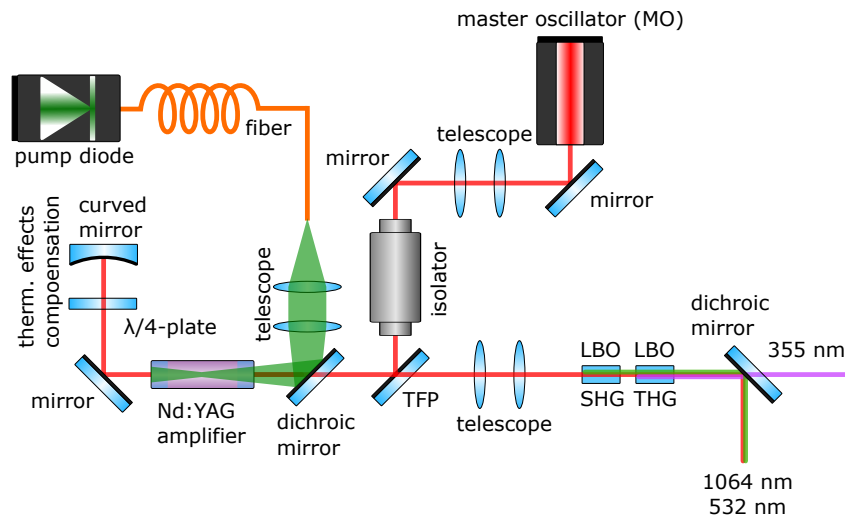


Fig. 1: Shown here is the second stage of the amplifier system. The MO is guided through a telescope to ensure best overlap in the amplifier rod. The beam is then guided through the amplifier rod after an isolator and 45° thin film polarizer (TFP). A quarter wave plate rotates the polarization after the second passage. Thermal lensing effects are compensated with a curved mirror. Due to three increasing doping concentrations within the diffusion bonded amplifier rod, it is end-pumped from only one side. After the double pass of the amplified MO beam it passes through the TFP and into a telescope to shape the beam for second/third harmonic generation (SHG/THG) in two LBO crystals. The desired wavelength is then separated with a suitable dichroic mirror.

rod from a thermally safe region. With these parameters we were able to amplify the MO to 1.4 mJ in double pass using a pump spot of around 1.1 mm in diameter and 1.8 mJ in single pass using a pump spot of 700 μm in diameter. Considering non-ideal overlap conditions this is well within what can be expected and confirms the pulse energies for successful frequency tripling can be reached.

The nonlinear LBO crystals for frequency tripling were tested with a similar source, but 3-10 mJ pulse energy at 100 Hz PRF. Efficiencies up to 28 % could be measured, which is more than enough to reach > 2.5 W in the final system.

4. Conclusion

In conclusion, we have built a MOPA demonstrator capable of being scaled to the needed pulse energy for direct wind detection in a GLA-based CAT-scenario. The latest state of the systems power scaling will be presented.

References

1. N. P. Schmitt, W. Rehm, T. Pistner, P. Zeller, H. Diehl, and P. Navé, "The awiator airborne lidar turbulence sensor," *Aerosp. Sci. Technol.* **11**, 546–552 (2007).
2. M. Wirth, A. Fix, P. Mahnke, H. Schwarzer, F. Schrandt, and G. Ehret, "The airborne multi-wavelength water vapor differential absorption lidar wales: system design and performance," *Appl. Phys. B* **96**, 201 (2009).
3. P. Vrancken, M. Wirth, G. Ehret, B. Witschas, H. Veerman, R. Tump, H. Barny, P. Rondeau, A. Dolfi-Bouteyre, and L. Lombard, "Flight tests of the DELICAT airborne LIDAR system for remote clear air turbulence detection," *EPJ Web Conf.* **119**, 14003 (2016).
4. O. Reitebuch, C. Lemmerz, E. Nagel, U. Paffrath, Y. Durand, M. Endemann, F. Fabre, and M. Chaloupy, "The airborne demonstrator for the direct-detection doppler wind lidar aladin on adm-aeolus. part i: Instrument design and comparison to satellite instrument," *J. Atmospheric Ocean. Technol.* **26**, 2501–2515 (2009).
5. B. Witschas, C. Lemmerz, A. Geiß, O. Lux, U. Marksteiner, S. Rahm, O. Reitebuch, and F. Weiler, "First validation of aeolus wind observations by airborne doppler wind lidar measurements," *Atmospheric Meas. Tech.* (2020).
6. P. Vrancken and J. Herbst, "Aeronautics application of direct-detection doppler wind lidar: An adapted design based on a fringe-imaging michelson interferometer as spectral analyzer," *Remote. Sens.* **14**, 3356 (2022).
7. O. Puncken, D. M. Gandara, M. Damjanic, P. Mahnke, R. B. Bergmann, M. Kalms, P. Peuser, P. Wessels, J. Neumann, and U. Schnars, "1 khz 3.3 μm nd: Yag ktioaso 4 optical parametric oscillator system for laser ultrasound excitation of carbon-fiber-reinforced plastics," *Appl. Opt.* **55**, 1310–1317 (2016).
8. L. M. Frantz and J. S. Nodvik, "Theory of pulse propagation in a laser amplifier," *J. Appl. Phys.* **34**, 2346–2349 (1963).
9. A. Ciapponi, W. Riede, G. Tzeremes, H. Schröder, and P. Mahnke, "Non-linear optical frequency conversion crystals for space applications," (2011).